Direct Numerical Simulation of Vortex Shedding Behind a Linearly Tapered Circular Cylinder

Vagesh D. NARASIMHAMURTHY[†], Helge I. ANDERSSON[†] and Bjørnar PETTERSEN[§]

[†]*Norwegian University of Science and Technology (NTNU), Department of Energy and Process Engineering, NO-7491 Trondheim, Norway, vagesh@ntnu.no*
[§]*NTNU, Department of Marine Technology, NO-7491 Trondheim, Norway*

Abstract. The three-dimensional transition to turbulence in the wake of a tapered circular cylinder with the taper ratio 75:1 has been analyzed by performing direct numerical simulation. The Reynolds number based on the uniform inflow velocity and the diameters at the wide and narrow ends were 300 and 102, respectively. The same Reynolds number range was previously studied by Parnaudeau et al. (*TSFP4*, 2005) but with a different taper ratio 40:1. The effect of taper ratio on the transition-turbulence was investigated in the present study and it was found that the Strouhal number *versus* Reynolds number curves nearly collapse. Thereby, indicating that a change in the taper ratio by a factor of two has only a modest effect on the Strouhal number. However, there still exists a significant contrast in the cellular shedding pattern. Flow-visualization of instantaneous λ_2-structures and the enstrophy $\mid \omega \mid$ revealed that the mode A appeared around $Re \approx 200$ and mode B around $Re \approx 250$.

Key words: instability, transition, turbulence, DNS, tapered cylinder.

1. Introduction

Three-dimensional flow over circular cylinders is a common phenomenon in many engineering applications which occurs behind oil-platform legs, chimneys, cooling towers and even tapered aircraft wings. Such three-dimensionalization of the separated flow is often induced by a spanwise variation of the cylinder diameter (e.g. tapered cylinders). A distinct feature of tapered cylinder wakes is that depending on the local Reynolds number (Re_{local}) along the span, a range of flow-regimes (e.g., laminar unsteady wake (L3), transition in the wake (TrW) or shear layer (TrSL), etc) may exist side by side in the same geometry. Three-dimensional instabilities in the wake of tapered circular cylinders (L3 regime) was previously studied by Papangelou [1], Piccirillo and Van Atta [2], Vallés et al. [3] and more recently by Narasimhamurthy et al. [4]. However, the TrW regime for tapered cylinders has had remarkably few investigations in comparison to uniform circular cylinders. Recently Parnaudeau et al. [5] performed Direct Numerical Simulation (DNS) in the TrW regime with a taper ratio, $R_T = l/(d_2 - d_1) = 40 : 1$ (where l is the length of the circular cylinder and d_2 and d_1 denote the diameter of its wide and narrow ends, respectively).

In the present study $R_T = 75 : 1$, which implies a more modest tapering than considered by Parnaudeau et al. [5] and the Reynolds numbers are same in both

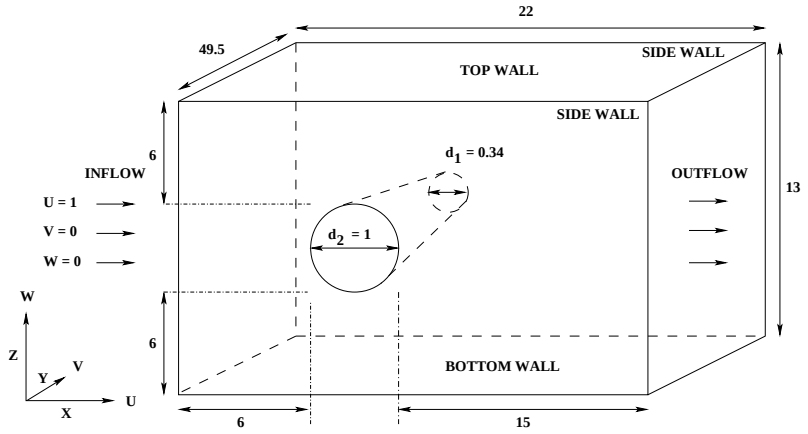

Figure 1. Computational domain (not to scale)

the cases. Thereby, the effect of tapering on the transition-turbulent process is investigated in the present study. In this DNS study, an in-depth exploration of the frequency spectra and the instantaneous vortical structures was carried out to understand both the evolution of large-scale structures (*vortex dislocation or vortex splits*) and the small-scale structures (*mode A and mode B*). Qualitative comparisons of the present results with the earlier numerical study in L3 regime [4], and in-house PIV (Particle Image Velocimetry) measurements by Visscher et al. [6] (where they studied TrSL regime) were also investigated.

2. Flow configuration and numerical method

The computational domain was as shown in Figure 1. All dimensions were normalized by d_2. The mean diameter, $d_m = 0.67$. The aspect ratio ($a = l/d_m$), R_T, and the Reynolds numbers Re_2, Re_1, Re_m, based on the uniform inflow velocity ($U = 1$) and the diameters d_2, d_1, d_m, respectively were as shown in Table 1.

Table 1. Flow parameters

Case	**a**	$\mathbf{R_T}$	$\mathbf{Re_2}$	$\mathbf{Re_1}$	$\mathbf{Re_m}$
Present simulation	74	75:1	300	102	201
Parnaudeau et al.[5]	40	40:1	300	100	200

The Navier-Stokes (N-S) equations in *incompressible* form were solved in 3-D space and time using a *parallel* Finite Volume code [4, 10]. The code uses staggered Cartesian grid arrangement. Time marching was carried out using a 3^{rd} order explicit Runge-Kutta scheme for the momentum equations and an iterative SIP (Strongly Implicit Procedure) solver for the Poisson equation. Spatial discretization was carried out using a 2^{nd} order central-differencing scheme. The total number of grid points used was equal to 15 x 10^6. The time step $\Delta t = 0.003 d_2/U$ and the number of Poisson iterations per time step was equal to 50.

A uniform inflow velocity profile $U = 1$ was fixed at the inlet without any free-stream perturbations. A *free-slip* boundary condition was applied on both the

side walls, top wall and the bottom wall (see Figure 1). At the outlet, Neumann boundary condition was used for velocities and pressure was set to zero. The *no-slip* boundary condition on the cylinder body was implemented by using a *direct forcing* Immersed Boundary Method (IBM) [4, 9]. The computations were performed on a *SGI Origin 3800* parallel computer. The total consumption of CPU-time was approximately equal to 12000 hours.

3. Results and discussion

3.1. FREQUENCY ANALYSIS

The time evolution of the instantaneous velocity components U, V, W and the instantaneous pressure, P, were sampled along two lines parallel to the axis of the cylinder and located $2d_m$ and $12d_m$ downstream the axis in X-direction, respectively. Both lines were offset by $1d_m$ in Z-direction. The time traces of U, V, W and P were plotted in Figure 2, 3, 4 and 5, respectively. The figures clearly indicate the oblique and cellular shedding pattern. Qualitative investigations of the frequency spectra were carried out by the spectral analysis of cross-stream velocity component (W) time trace. In Figure 6(a) the Strouhal number ($St = fd_m/U$) *versus* Re_{local} ($= Ud_{local}/\nu$; d_{local} is the local diameter) curve from Parnaudeau et al. [5] was compared against the present result. It is surprising to see that the curves nearly collapse. Thereby, indicating that a change in the R_T by a factor of two doesn't affect the Strouhal number much. However, there still exists a significant contrast in the distribution of constant-frequency cells along the span.

The vortex dislocations in the TrW state of flow of a uniform circular cylinder typically occurs at the location of mode A instability [8]. In contrast, these large-scale structures occur spontaneously along the whole span for tapered circular cylinders (see Figure 6(b)). The two discontinuities in the local Strouhal number ($St_{local} = fd_{local}/U$) *versus* Re_{local} curve in Figure 6(b) for the uniform circular cylinder correspond to change over of eddy-shedding mode from laminar-mode A and mode A-mode B, respectively [8]. However, for the tapered case it seems that the vortex dislocations depend primarily on the R_T.

In Figure 7 the St_{local} curve from the present simulation (TrW regime) was plotted together with the results from Narasimhamurthy et al. [4] (L3 regime) and the PIV measurements by Visscher et al. [6] (TrSL regime). In all the three studies $R_T = 75 : 1$. The Strouhal number initially increases with Reynolds number and then decreases with the increase in Re_m, similar to the uniform circular cylinder [11]. Piccirillo and Van Atta [2] in their experimental study (L3 regime) observed that the shedding cell size increases with the local diameter. A similar observation was also reported by Parnaudeau et al. [5]. In Figure 7 it can be seen that shedding cell size clearly increases towards the large diameter for low-Reynolds numbers (L3 and TrW). It seems that this observation is only valid for low-Reynolds numbers as the curves for TrSL doesn't follow this trend.

3.2. INSTANTANEOUS VORTICAL STRUCTURES

In order to identify the topology and the geometry of the vortex cores correctly the λ_2-definition by Jeong and Hussain [12] was used. λ_2 corresponds to the second

largest eigenvalue of the symmetric tensor $S_{ij}S_{ij} + \Omega_{ij}\Omega_{ij}$, where S_{ij} and Ω_{ij} are respectively the symmetric and antisymmetric parts of the velocity gradient tensor. Figure 8 shows the iso-surfaces of negative λ_2 at different instances in time, t. 3-dimensionality in the form of waviness in the spanwise vortex cores (primary Karman vortices) is evident even in the L3 regime. The snap shots clearly illustrate the time-evolution of the vortex dislocations (around $Y = 25 - 40$) and the small-scale streamwise structures (mode A and mode B) along the span. However, vortex dislocations are more clearly visible in Figure 9. Negative λ_2, vorticity magnitude or enstrophy $\mid \omega \mid$ and the vorticity components evaluated at the same instant in time were plotted together. The vortex dislocations formed between spanwise cells of different frequency when the primary vortices move out of phase with each other are visible at $Y \approx 12, 23, 40$. The development of helical twisting of vortex tubes is visible in the vicinity of the vortex dislocations. Williamson [7] concluded that these helical twistings are the fundamental cause for the rapid spanwise spreading of dislocations, and indeed for the large-scale distortion and break-up to turbulence in a natural transition wake.

In uniform circular cylinder wakes the Reynolds number will be constant along the whole span and therefore the individual modes of 3-dimensionality (either mode A or mode B) exist along the entire span of the cylinder. Barkley and Henderson [13] from their Floquet stability analysis predicted the critical Reynolds number for the uniform circular cylinder to be 188.5 ± 1.0 and the wavelength of mode A equal to 3.96 diameters. However, in the present tapered cylinder study the Re_{local} varies along the span and both mode A and mode B co-exists in the same geometry. Thereby, only a small span of the cylinder is available for each of the modes to develop (especially for mode A) and it is hard to pin-point the exact Reynolds number at which these modes start to appear. Parnaudeau et al. [5] reported that the mode A behind their tapered cylinder occurred in the L3 regime. Flow-visualization of the present DNS revealed that the mode A appeared around $Re_{local} \approx 200$ and mode B around $Re_{local} \approx 250$.

4. Conclusions

The effect of taper ratio on the transition-turbulence was investigated in the present study and it was found that the Strouhal number *versus* Reynolds number curves nearly collapse. Thereby, indicating that a change in the taper ratio by a factor of two doesn't affect the Strouhal number much. However, there still exists a significant contrast in the cellular shedding pattern.

Spot-like vortex dislocations in the TrW regime of uniform circular cylinders correspond to change over of eddy-shedding mode from laminar-mode A and mode A-mode B [8] but for tapered circular cylinders it primarily depends on R_T. In the present investigation, it was observed that the shedding cell size increases with the local diameter, which is in agreement with the previous studies at low-Reynolds numbers [2, 4, 5]. Both mode A and mode B were found to co-exist in the same geometry but only in a small span of the cylinder. It was hard to pin-point the exact Reynolds number at which these modes develop. However, from the flow-visualization it can be concluded that the mode A appeared around $Re_{local} \approx 200$ and mode B around $Re_{local} \approx 250$.

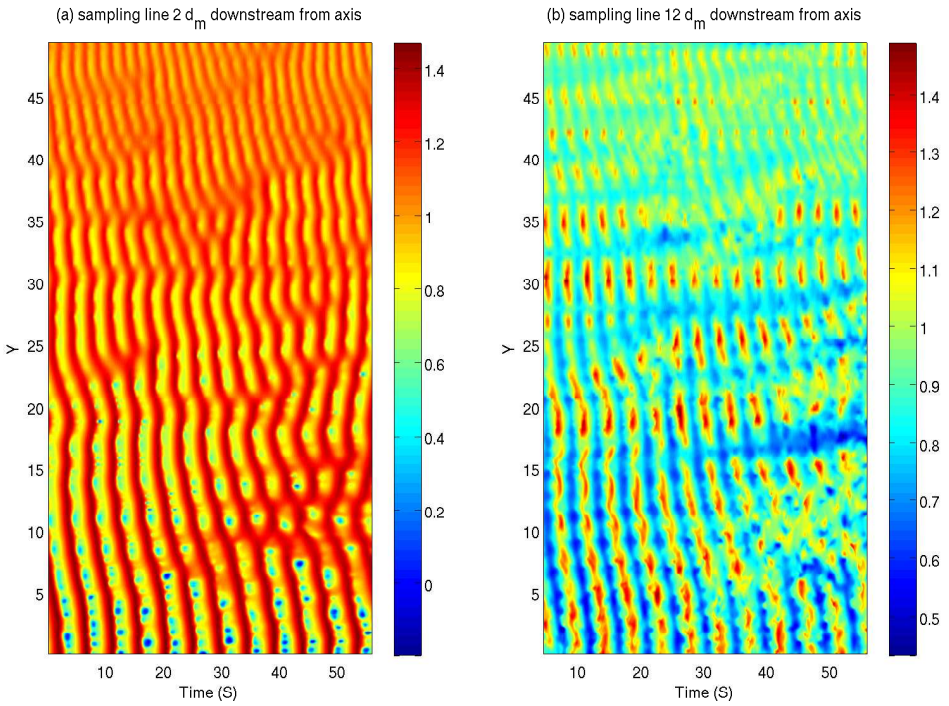

Figure 2. Time evolution of the U velocity along the entire span. Y = 0 corresponds to Re_2 and Y = 49.5 corresponds to Re_1.

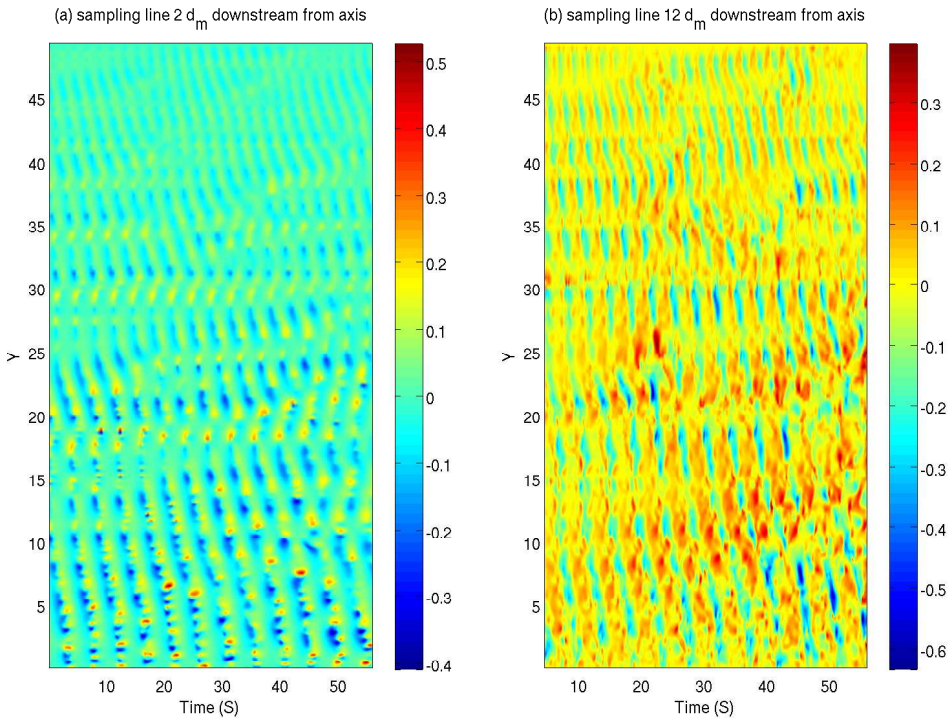

Figure 3. Time evolution of the V velocity along the entire span (see Figure 2 for details).

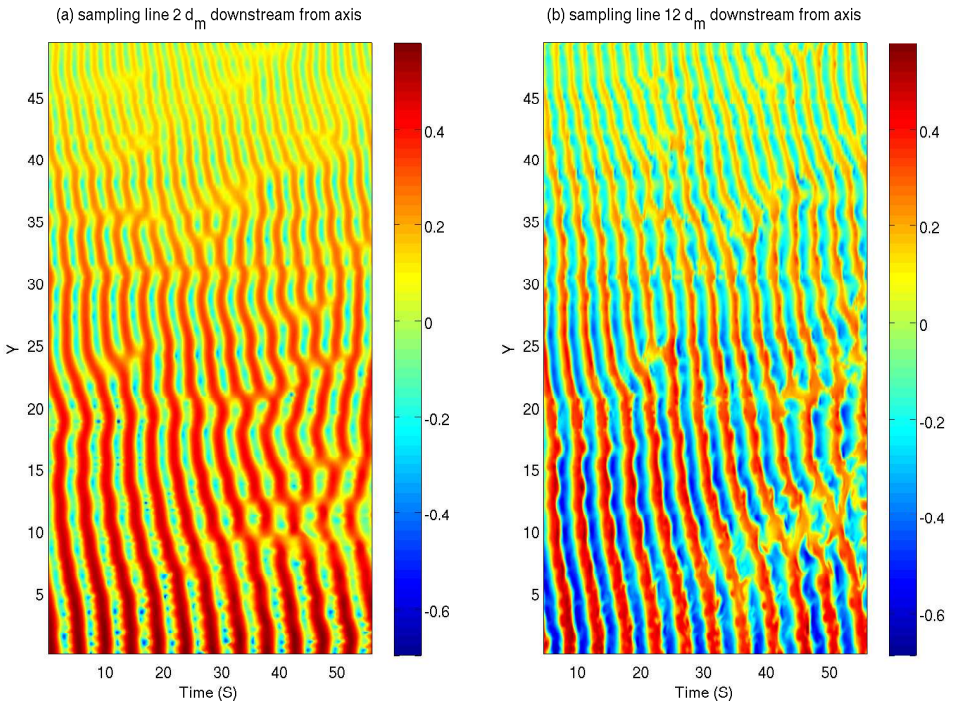

Figure 4. Time evolution of the W velocity along the entire span (see Figure 2 for details).

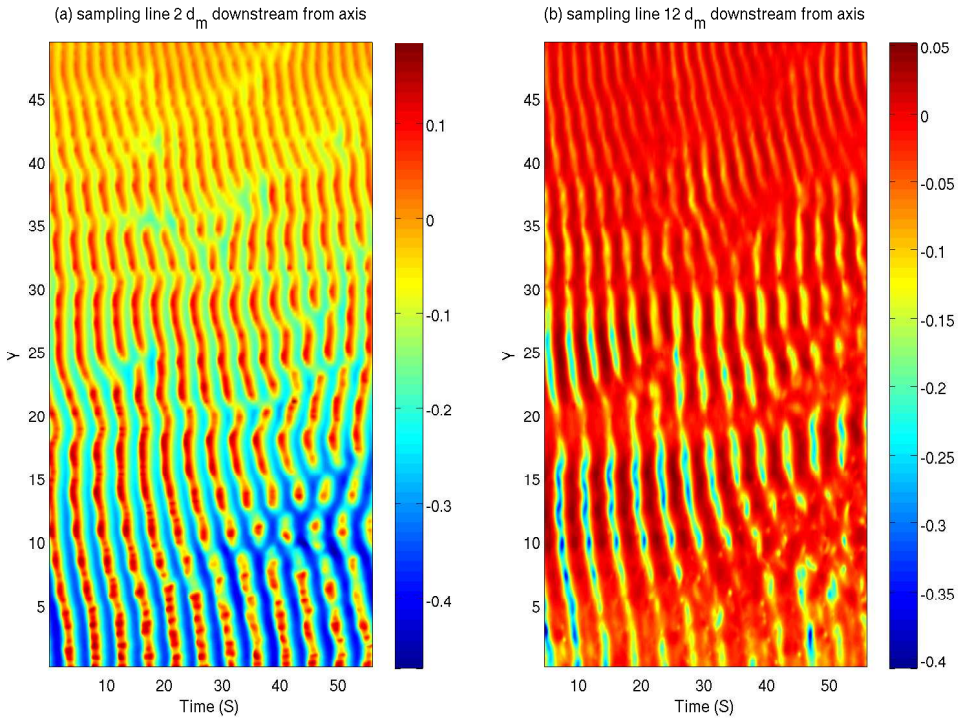

Figure 5. Time evolution of the Pressure P along the entire span (see Figure 2 for details).

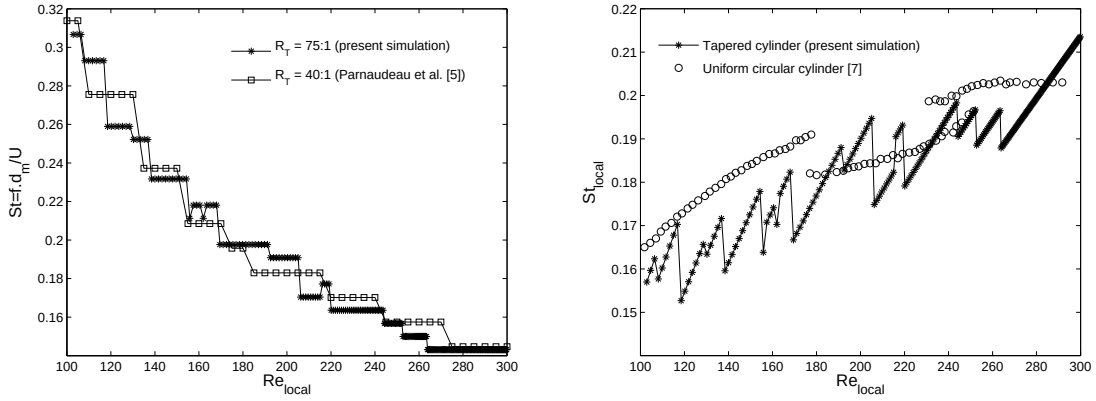

(a) Effect of taper ratio (R_T) (b) Tapered cylinder *versus* uniform circular cylinder

Figure 6. Strouhal number *versus* Reynolds number.

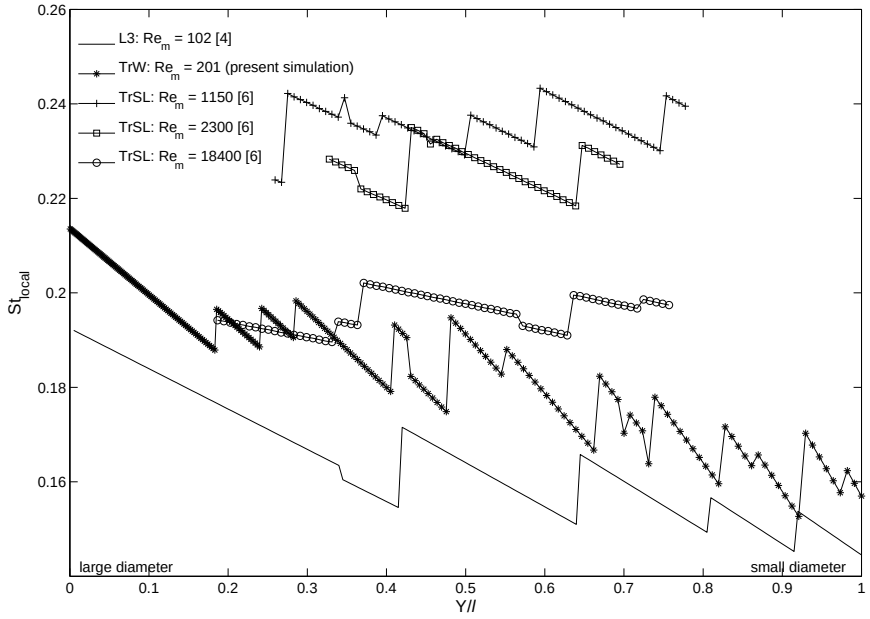

Figure 7. St_{local} along the non-dimensionalized span. $R_T = 75:1$ for all the curves.

Acknowledgments

This work has received support from The Research Council of Norway (Programme for Supercomputing) through a grant of computing time. The first author was the recipient of a research fellowship offered by The Research Council of Norway.

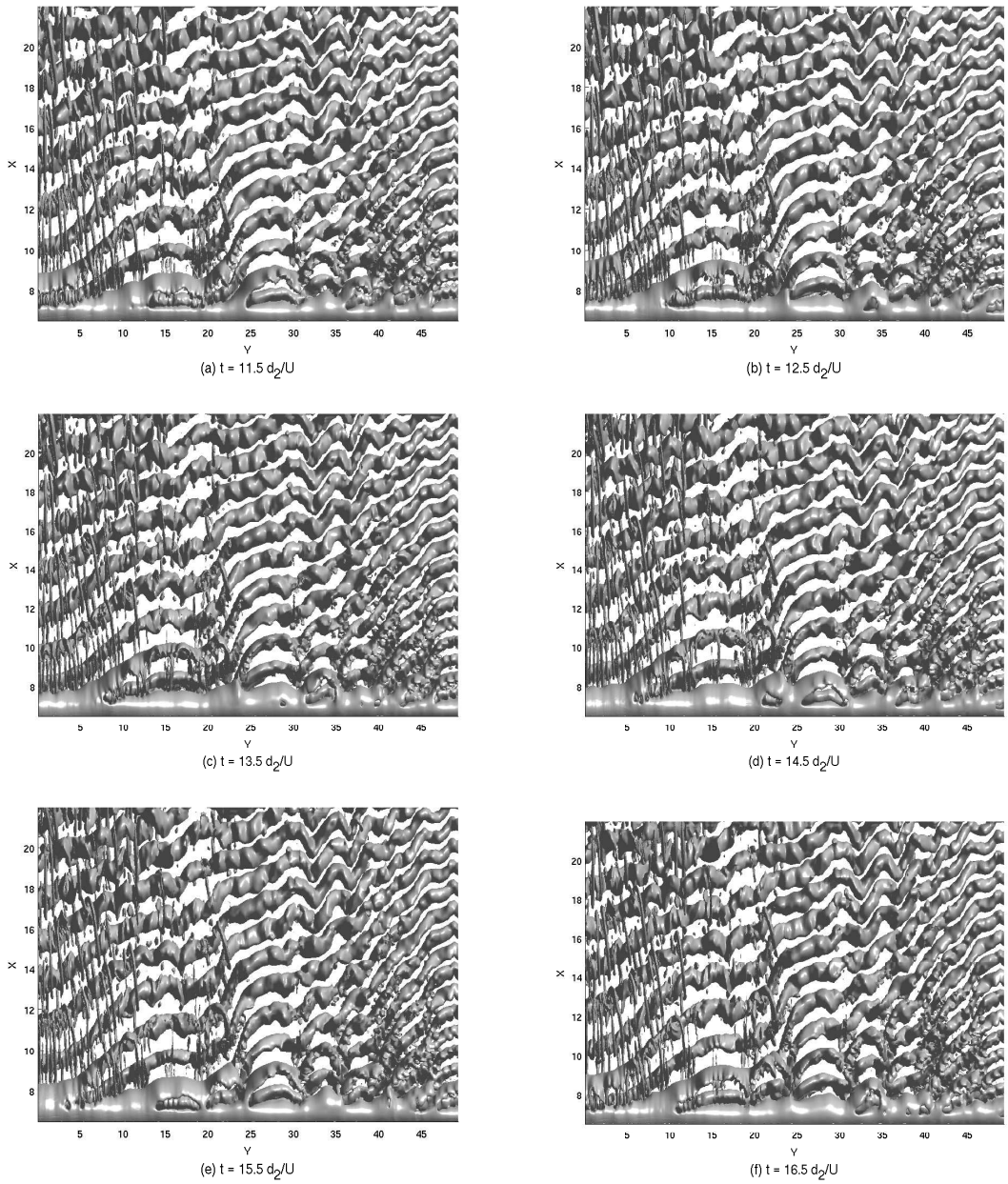

Figure 8. 3-dimensional λ_2 contours (negative λ_2) showing the topology and geometry of the vortex cores at different instances in time, t. Y-axis corresponds to the axis of the cylinder. The flow direction is from bottom to top.

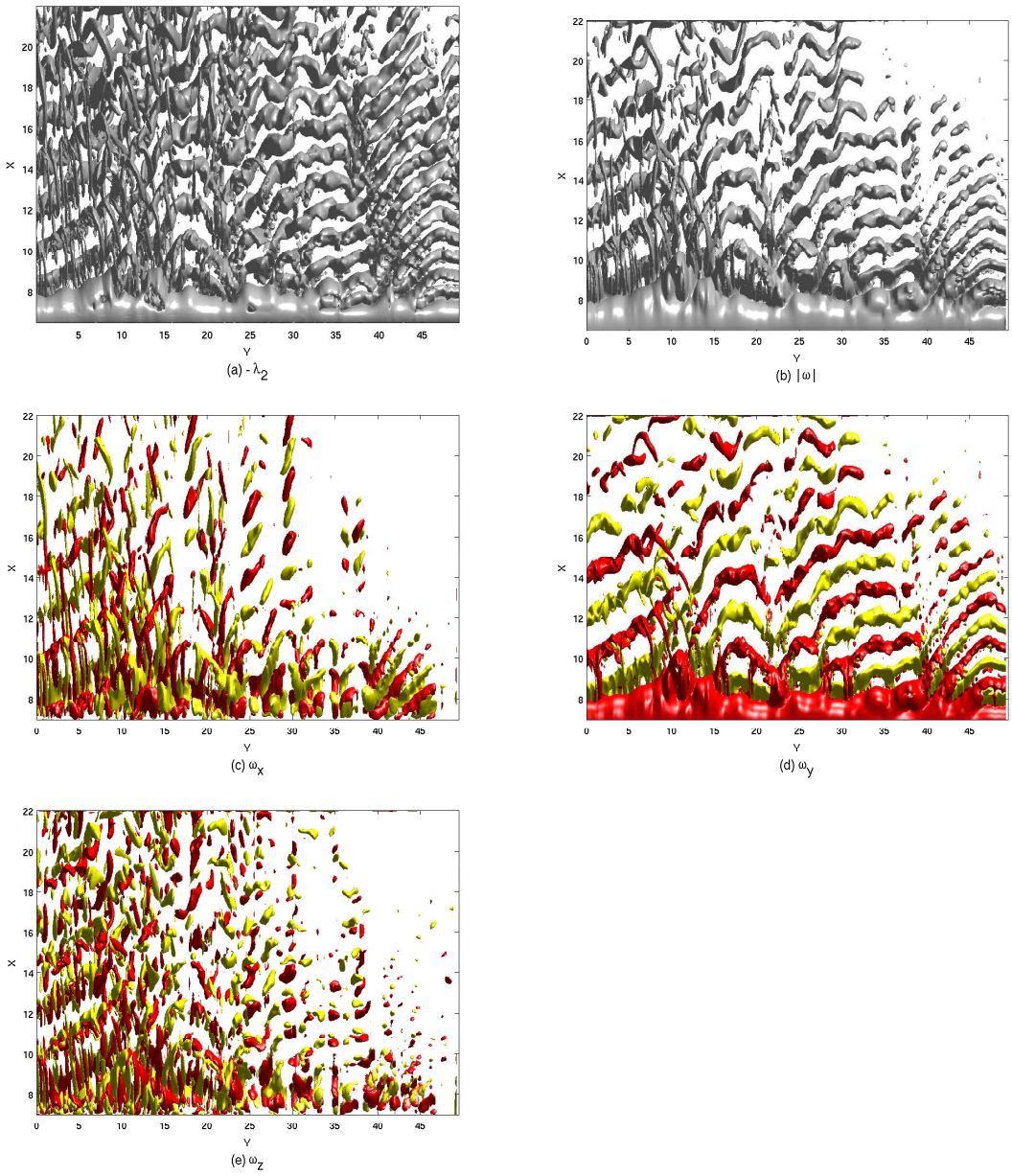

Figure 9. 3-dimensional vortical structures at the same instant in time, $t = 47d_2/U$ as vortex dislocation occurs along the span. The flow direction is from bottom to top. (a)Negative λ_2; (b)Enstrophy $\mid \omega \mid$; (c)streamwise vorticity ω_x; (d)spanwise vorticity ω_y; (e)cross-stream vorticity ω_z. The surfaces colored yellow and red mark a particular value of positive and negative vorticity, respectively.

References

[1] Papangelou, A., Vortex shedding from slender cones at low Reynolds numbers. *J. Fluid Mech.* **242**, (1992), 299-321.

[2] Piccirillo, P. S. and Van Atta, C. W., An experimental study of vortex shedding behind linearly tapered cylinders at low Reynolds number. *J. Fluid Mech.* **246**, (1993), 163-195.

[3] Vallès, B., Andersson, H. I. and Jenssen, C. B., Oblique vortex shedding behind tapered cylinders. *J. Fluids Struct.* ***16***, (2002), 453-463.

[4] Narasimhamurthy, V. D., Schwertfirm, F., Andersson, H. I. and Pettersen, B., Simulation of unsteady flow past tapered circular cylinders using an immersed boundary method. In: *Proc. ECCOMAS Computational Fluid Dynamics 06*, Eds. P. Wesseling, E. Oñate, J. Périaux, Publisher TU Delft, The Netherlands, Egmond aan Zee (2006).

[5] Parnaudeau, P., Heitz, D., Lamballais, E. and Silvestrini, J. H., Direct numerical simulations of vortex shedding behind cylinders with spanwise linear nonuniformity. In: *Proc. Turbulence and Shear Flow Phenomena 4*, USA, Virginia (2005) 111-116.

[6] Visscher, J., Pettersen, B. and Andersson, H. I., PIV study on the turbulent wake behind tapered cylinders. In: *Proc. EUROMECH European Turbulence Conference 11*, Portugal, Porto (2007).

[7] Williamson, C. H. K., The natural and forced formation of spot-like vortex dislocations in the transition of a wake. *J. Fluid Mech.* **243**, (1992), 393-441.

[8] Williamson, C. H. K., Vortex dynamics in the cylinder wake. *Annu. Rev. Fluid. Mech.* **28**, (1996), 477-539.

[9] Peller, N., Le Duc, A., Tremblay F. and Manhart M., High-order stable interpolations for immersed boundary methods. *Int. J. Numer. Meth. Fluids.* **52**, (2006), 1175-1193.

[10] Manhart M., A zonal grid algorithm for DNS of turbulent boundary layers. *Computers & Fluids.* **33**, (2004), 435-461.

[11] Zdravkovich, M. M., *Flow Around Circular Cylinders: Volume 1*, Oxford Univ. Press, (1997).

[12] Jeong, J. and Hussain, F., On the identification of a vortex. *J. Fluid Mech.* **285**, (1995), 69-94.

[13] Barkley, D. and Henderson, R. D., Three-dimensional Floquet stability analysis of the wake of a circular cylinder. *J. Fluid Mech.* **322**, (1996), 215-241.